

## Thickness Measurement of Surface Layer by the Angular Dependent X-Ray Photoelectron Spectroscopy

Masamichi YAMADA and Haruo KURODA\*

Department of Chemistry, Faculty of Science, The University of Tokyo, Hongo, Tokyo 113

(Received December 19, 1979)

A sample-holding device to study the photoelectron take-off angle dependence of XPS spectrum is described. The take-off angle dependence was studied on a silicon surface covered with an oxide layer and a contamination carbon layer, and the (thickness)/(electron attenuation length) ratio of each layer was determined from the analysis of the angular dependence of the Si2p, O1s, and C1s peak intensities.

An ordinary solid surface is often covered with an oxide layer, adsorbed materials, and so on. It is well known that the contribution from the surface layer to the XPS spectrum is enhanced while that from the substrate is depressed as the photoelectron take-off angle  $\theta$  measured from the specimen surface is decreased, provided that the specimen has an atomically flat surface.<sup>1,2)</sup> This method is useful to distinguish the photoelectron peaks due to the surface layer from those due to the substrate. Furthermore, the thickness of the surface layer  $t$  or the electron attenuation length  $\Lambda$  can be determined from the quantitative analysis of the angular dependent peak intensities.<sup>1,2)</sup>

For such an analysis, it is necessary to measure signal intensities at various different photoelectron take-off angles ranging from nearly zero degree to about ninety degrees. As described later, it is predicted that the angular variation of the absolute peak intensity is determined by the (thickness)/(electron attenuation length) ratio  $t/\Lambda$  under the idealized experimental conditions.<sup>1)</sup> However, this prediction has been experimentally verified only in few cases.<sup>1,3)</sup> In most of angular dependent XPS studies performed so far, the angular variation of peak intensity was largely modified by instrumental factors such as an inhomogeneous X-ray flux,<sup>4)</sup> a finite sample size and the misalignment of a sample, and consequently the observed total signal intensity decreased markedly at low take-off angles.<sup>4,5)</sup> In such a case, instead of the absolute intensities, the angular dependence of the intensity ratios between photoelectron peaks of the same specimen had to be used in the analysis in order to cancel out the effect of the angular dependent instrumental factors.<sup>2)</sup>

In this report, we describe a rather simple sample rotation device which is incorporated into a McPherson ESCA 36 photoelectron spectrometer. The utility of the device is verified by the results obtained on a silicon surface covered with oxide and contamination carbon layers. Further, the results show that, in a measurement carried out with the device, the angular variation of signal intensities can be analyzed to determine  $t/\Lambda$  values without any correction and without resort to intensity ratios.

### Variable-angle Sample Holder

The electron energy analyzer of a McPherson ESCA 36 spectrometer is composed of two concentric spherical sectors of 360 mm mean radius, without any retarding lens system. The X-ray source and sample-treatment

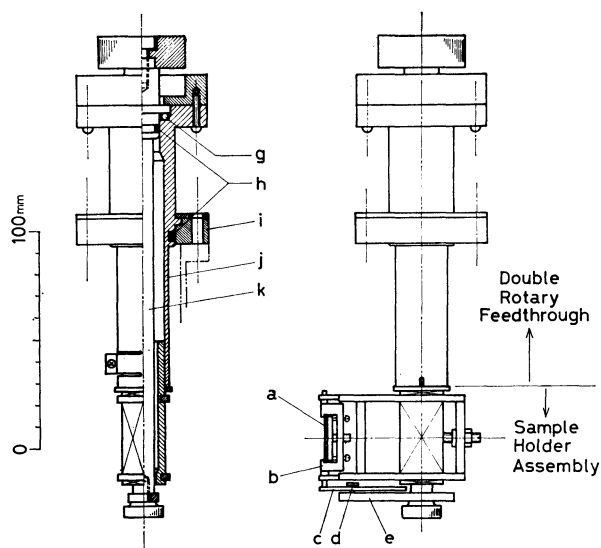


Fig. 1. Variable-angle sample-holding device.

(a): Sample, (b): sample holder, (c): "tail" of sample holder, (d): pin, (e): arm, (g): stainless steel balls, (h): O-rings, (i): flange, (j): outer tube, (k): central shaft. (In the left drawing, the sample holder is omitted for brevity.)

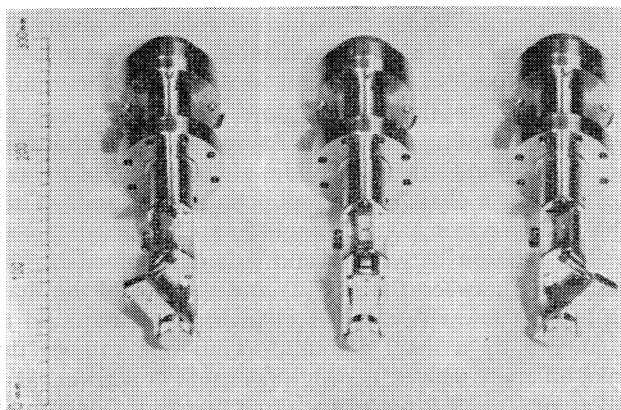


Fig. 2. Photographs showing the sample-holding device at three different sample orientations. From left to right, the photoelectron take-off angle  $\theta$  is set to be ca. 10°, 45°, and ca. 80°, respectively.

devices are incorporated into the sample chamber.

Figure 1 illustrates full details of the variable-angle sample holding device. Its photographs are shown in Fig. 2. The device consists of two parts; a sample holder assembly and an O-ring-sealed double rotary

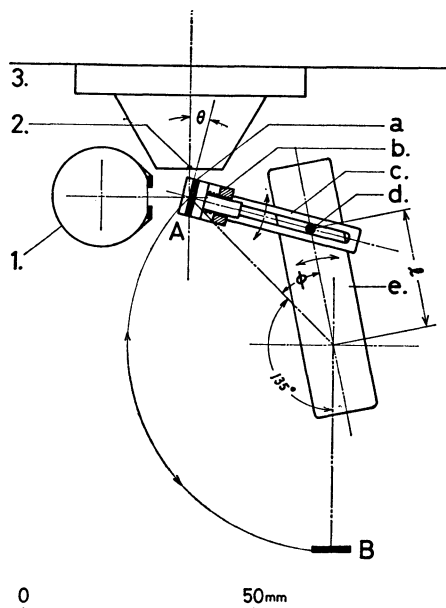


Fig. 3. Working principle of the variable-angle sample holder.

A: XPS measurement position, B: sample-treatment position, 1: X-ray source, 2: entrance slit, 3: analyzer chamber wall,

(a): sample, (b): sample holder, (c): "tail" of sample holder, (d): pin, (e): arm. (Each corresponding part is designated by the same letter as in Fig. 1.)

feedthrough which is composed of an outer tube (j) and a central shaft (k). The sample holder assembly is clamped to the outer tube (j), and can be rotated within the sample chamber by rotating the outer tube (j) from the outside. By this motion, the sample can be transferred between the measuring position (A) and the position (B) for sample deposition, argon-ion etching, and other sample treatments (see Fig. 3). In the sample holder assembly, a tail (c) is attached to the bottom of the sample holder (b) which is rotatable about the vertical axis lying in the specimen surface. The arm (e) is firmly fixed to the central shaft (k) of the rotary feedthrough so that the angle  $\phi$  (in Fig. 3) can be varied by rotating the latter. As the angle  $\phi$  is changed, the pin (d) on the arm (e) slides along the slit of the tail (c) causing a change of the direction of the tail. Thus the photoelectron take-off angle  $\theta$  can be varied.

The relation between  $\theta$  and  $\phi$  is determined by the distance  $l$  between the pin (d) and the axis of the shaft (k). At a lower  $\theta$ , a larger change of  $\phi$  is required to change  $\theta$  by a fixed amount. Thus one can set the take-off angle with rather high precision at a lower take-off angle. This is one of the great merits of this sample rotation mechanism. The pin (d) can be placed at one of the three positions on the arm (e) depending on the range of  $\theta$  to be studied. Because of the narrow width (0.25 mm) of the entrance slit of the analyzer, the mispositioning of a specimen results in the large decrease of signal intensity at low  $\theta$ . In the case of this device, monitoring the counting rate, we can set the specimen in the optimum position by adjusting the rotation of the outer tube (j), and thus prevent the deformation of the angular dependence. This is another

merit of this device.

### Angular Dependent XPS Spectrum of a Silicon Wafer

We examined the angular dependence of the XPS spectrum of a silicon wafer with a polished (100) face. The wafer had been kept for a long time in the ordinary atmosphere without any oxidation treatment. The sample of the size 8 mm  $\times$  21 mm was cut out from the wafer, and ultrasonically washed in organic solvents, distilled water, and finally trichloroethylene. After air-dried, the sample was transferred into the sample chamber of the McPherson ESCA 36 spectrometer. The XPS measurements were performed with Mg  $K\alpha$  (1253.6 eV) radiation (7.4–7.5 kV, 25–27 mA) under the vacuum better than  $10^{-4}$  Pa produced by a turbomolecular pump. The take-off angle was varied successively from the highest ( $78^\circ$ ) to the lowest ( $3^\circ$ ) and finally again set at  $78^\circ$ . As compared with the initial measurement at  $78^\circ$ , the intensity obtained by the final measurement at the same angle was found to be slightly higher for all photoelectron peaks, which was probably due to the slight increase of the X-ray flux.

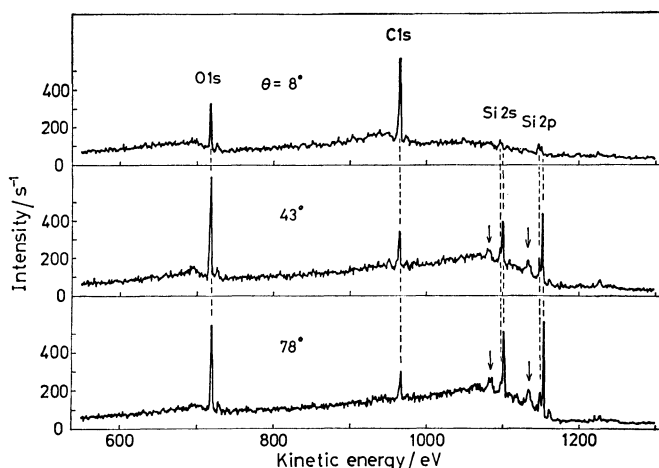


Fig. 4. Wide-scan spectra of a silicon wafer. The spectra were measured at the take-off angles,  $78^\circ$ ,  $43^\circ$ , and  $8^\circ$ . Both Si2p and Si2s peaks are accompanied by loss peaks due to plasmon excitation (indicated by arrows).

Figure 4 shows the wide-scan spectra obtained at three different take-off angles,  $8^\circ$ ,  $43^\circ$ , and  $78^\circ$ . The spectrum at  $\theta=78^\circ$  shows strong peaks attributable to Si2p, Si2s, and O1s, and a weak peak attributable to C1s. Both the Si2p and Si2s peaks are accompanied by energy-loss peaks. On decreasing  $\theta$ , the intensities of the Si2p and Si2s peaks decrease, but that of the C1s peak increases. As can be seen in Fig. 4, the angular variation of the O1s peak intensity is different from the others. The narrow-scan spectra of the Si2p region are shown in Fig. 5, in which the higher kinetic energy peaks are due to elemental silicon and the lower kinetic energy ones are due to oxidized silicon.<sup>6)</sup> Note that the angular dependence is different between these two components.

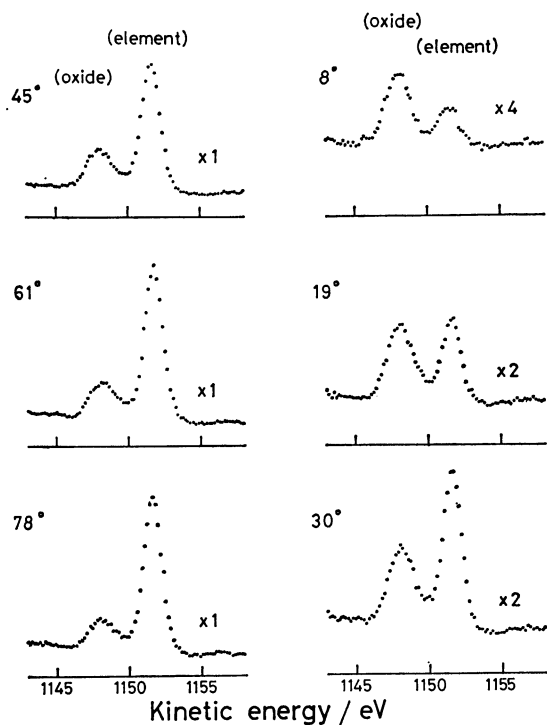


Fig. 5. Variation of the Si2p spectrum as the take-off angle changes from 78° to 8°. The higher kinetic energy peaks are due to elemental silicon and the lower kinetic energy ones are due to oxidized silicon.

Net intensities (peak height above background) of the Si2p(element), Si2p(oxide), O1s, and C1s peaks are plotted in Fig. 6 as a function of  $\theta$ . We can clearly see that the  $\theta$  dependences of the Si2p(oxide) and O1s peak intensities are very similar to each other, indicating that the observed O1s peak is entirely due to the silicon oxide. Thus we take the model that the silicon surface is covered with an oxide layer of the uniform thickness  $t_2$

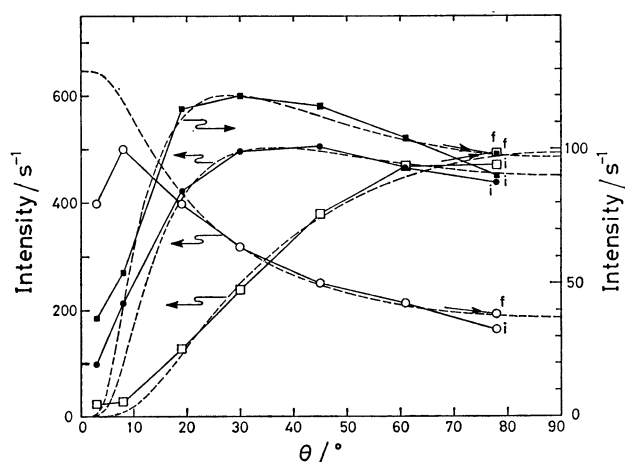


Fig. 6. Angular dependence of C1s (○), O1s (●), Si2p (oxide) (■), and Si2p (element) (□) peak intensities (by net peak height).

At  $\theta=78^\circ$ , the points designated by "i" and "f" represent the intensities obtained by the initial and final measurements, respectively. Broken lines represent the angular variations calculated for the model illustrated in Fig. 7 by using the  $t/A$  values in Table 1.

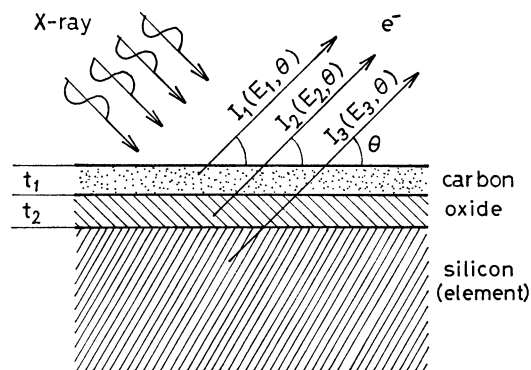


Fig. 7. Model for the surface region of the silicon wafer.  $I_1(E_1, \theta)$ ,  $I_2(E_2, \theta)$ , and  $I_3(E_3, \theta)$  are the contributions from the top-most contamination carbon layer, from the silicon oxide layer, and from the elemental silicon substrate, respectively.

and a contamination carbon layer of the thickness  $t_1$ , as illustrated in Fig. 7.<sup>7)</sup> We will assume also that no oxygen-containing species is included in the contamination carbon layer. As discussed by Fadley *et al.*,<sup>1)</sup> on the assumptions that (a) the specimen surface is atomically flat, (b) the X-ray flux is uniformly distributed over the whole sample area, and (c) the specimen volume included in the acceptance area of the analyzer contributes uniformly to the spectrum and the portion outside the acceptance area does not contribute, the following expressions are derived for the intensity  $I(E, \theta)$  of the peak (at the kinetic energy  $E$ ) measured at the take-off angle  $\theta$ :

$$I_1(E_1, \theta) = I_1^0 [1 - \exp\{-t_1/A_1(E_1) \sin \theta\}] \quad (1)$$

for the C1s peak ( $E_1=966$  eV) due to the top-most layer,

$$I_2(E_2, \theta) = I_2^0 [1 - \exp\{-t_2/A_2(E_2) \sin \theta\}] \times \exp\{-t_1/A_1(E_2) \sin \theta\} \quad (2)$$

for the Si2p(oxide) ( $E_2=1150$  eV) and O1s ( $E_2=718$  eV) peaks due to the oxide layer, and

$$I_3(E_3, \theta) = I_3^0 \exp\{-t_2/A_2(E_3) \sin \theta\} \times \exp\{-t_1/A_1(E_3) \sin \theta\} \quad (3)$$

for the Si2p(element) peak ( $E_3=1150$  eV) due to the bulk.  $A_1(E)$  and  $A_2(E)$  are the electron attenuation lengths of the photoelectrons with kinetic energy  $E$  in the carbon and oxide layers respectively, and  $I_1^0$ ,  $I_2^0$ , and  $I_3^0$  are constants independent of  $\theta$ . Equation 3 can be rewritten as follows:

$$I_3(E_3, \theta) = I_3^0 \exp\left[-\left\{\frac{t_1}{A_1(E_3)} + \frac{t_2}{A_2(E_3)}\right\} \frac{1}{\sin \theta}\right] \quad (3')$$

Thus  $I_3(E_3, \theta)$  is expected to be exponentially dependent on  $1/\sin \theta$ . The observed angular dependence of the Si2p(element) peak intensity was found to be well described by Eq. 3' by using the following value:

$$\frac{t_1}{A_1(E_3)} + \frac{t_2}{A_2(E_3)} = 0.68 \quad (E_3=1150 \text{ eV}).$$

In the photoelectron kinetic energy range concerned here,  $A(E)$  can be considered to be nearly proportional to  $E^{1/2}$ .<sup>8)</sup> If we adopt the relation that  $A(E)=A(E_3) \cdot (E/E_3)^{1/2}$ , we can treat either  $t_1/A_1(E_3)$  or  $t_2/A_2(E_3)$  as the only one adjustable parameter, and determine its

TABLE 1.  $t/\lambda$  VALUES DERIVED FROM THE ANALYSIS OF THE EXPERIMENTAL ANGULAR DEPENDENCE

	$E/\text{eV}^{\text{a)}}$	$t_1/\lambda_1(E)^{\text{b)}}$	$t_2/\lambda_2(E)^{\text{c)}}$
Cl <sub>1s</sub>	966	0.34	—
O <sub>1s</sub>	718	0.39	0.47
Si <sub>2p</sub>	1150	0.31	0.37

a) Approximate kinetic energy. b) The (thickness)/(electron attenuation length) ratio for the top-most contamination carbon layer. The relation  $\lambda_1(E) \propto E^{1/2}$  is assumed. c) The (thickness)/(electron attenuation length) ratio for the oxide layer. The relation  $\lambda_2(E) \propto E^{1/2}$  is assumed.

value so that the observed take-off angle dependences of other photoelectron peak intensities can be well reproduced by using Eq. 1 or Eq. 2. The  $t/\lambda$  values thus obtained are listed in Table 1, and the angular dependence which is calculated for each peak by using these  $t/\lambda$  values is shown in Fig. 6 with a broken line. The agreement between the observed and calculated angular dependences is very satisfactory for all peaks, except at angles below  $10^\circ$ . The above discrepancy at low angles may be attributed to the effect of small roughness of the surface.<sup>9)</sup>

As described above, the angular-dependent XPS spectrum of a silicon wafer surface obtained with our variable-angle sample holder can be very satisfactorily explained by using Eqs. 1—3 on the model shown in Fig. 7. The  $\lambda$  value at  $E=1382$  eV (Si<sub>2p</sub> photoelectrons excited by Al  $K\alpha$ ) in SiO<sub>2</sub> was reported to be  $3.7 \pm 0.4$  nm.<sup>7)</sup> If we take this value, the thickness of the oxide layer of the present sample is estimated to be about 1.2 nm from the value  $t_2/\lambda_2(1150 \text{ eV})=0.37$ .<sup>10)</sup> Since we have not given any special oxidation treatment, this value may be considered as the typical thickness of the oxide layer that exists on the polished surface of a silicon wafer after prolonged exposure to the air, and it is in good agreement with the value  $<1.4$  nm reported by Raider *et al.*<sup>11)</sup> from fixed-angle XPS experiments. We do not know the materials contained in the contamination carbon layer, but most of them are likely to be hydrocarbons since the assumption that photoelectrons from the top-most layer does not contribute to the O<sub>1s</sub> peak intensity is supported by the above analysis of the angular dependent data. The electron attenuation length in a hydrocarbon layer was derived to be about 3.6 nm at  $E=1117$  eV.<sup>12)</sup> Thus from the value  $t_1/\lambda_1(1150 \text{ eV})=0.31$ , the thickness of the contamination carbon layer is estimated to be about 1.1 nm.

The authors wish to express their thanks to Dr. Katsuro Sugawara of Hitachi Ltd. for kindly supplying the silicon wafer used in the present study. We also would like to thank Dr. Isao Ikemoto, the University of Tokyo, for his helpful discussions.

## References

- 1) C. S. Fadley, R. J. Baird, W. Siekhaus, T. Novakov, and S. Å. L. Bergström, *J. Electron Spectrosc. Relat. Phenom.*, **4**, 93 (1974).
- 2) C. S. Fadley, *Prog. Solid State Chem.*, **11**, 265 (1976), and references therein.
- 3) W. A. Fraser, J. V. Florio, W. N. Delgass, and W. D. Robertson, *Surf. Sci.*, **36**, 661 (1973).
- 4) R. J. Baird and C. S. Fadley, *J. Electron Spectrosc. Relat. Phenom.*, **11**, 39 (1977).
- 5) For example, R. O. Ansell, T. Dickinson, A. F. Povey, and P. M. A. Sherwood, *J. Electron Spectrosc. Relat. Phenom.*, **11**, 301 (1977).
- 6) It is claimed that thin oxide films ( $<2.0$  nm) on silicon substrates are not stoichiometric SiO<sub>2</sub> but of nonstoichiometric nature containing silicon atoms in lower oxidation states. (See for example: S. I. Raider and R. Flitsch, *IBM J. Res. Develop.*, **22**, 294 (1978); D. E. Aspnes and J. B. Theeten, *Phys. Rev. Lett.*, **43**, 1046 (1979).) Also in this study, a Si<sub>2p</sub>(oxide) peak is broader than a Si<sub>2p</sub>(element) peak, and exhibits tailing towards higher kinetic energies (Fig. 5,  $\theta=19^\circ$ ).
- 7) An angular-dependent XPS study on oxidized silicon wafers has been performed by Hill *et al.* with a modified Hewlett-Packard 5950A spectrometer. (J. M. Hill, D. G. Royce, C. S. Fadley, L. F. Wagner, and F. J. Grunthaner, *Chem. Phys. Lett.*, **44**, 225 (1976).) Based on the same model as shown in Fig. 7, they analyzed the angular variation of the Si<sub>2p</sub>(oxide)/Si<sub>2p</sub>(element) intensity ratio.
- 8) C. J. Powell, *Surf. Sci.*, **44**, 29 (1974).
- 9) The observed Cl<sub>1s</sub> signal intensity at  $\theta=3^\circ$  does not lie on the smoothly extrapolated line. At  $\theta=3^\circ$ , the specimen stands nearly perpendicularly in front of the entrance slit. Therefore, when viewed from the entrance slit, the area occupied by the specimen surface becomes smaller than the acceptance area of the analyzer. This is likely to be the reason for the deviation from the curve at  $\theta=3^\circ$  (see Ref. 1).
- 10) It is necessary to take into account the difference between the kinetic energies of photoelectrons excited by Mg  $K\alpha$  and Al  $K\alpha$ . The  $\lambda$  value at  $E=1150$  eV in SiO<sub>2</sub> is estimated to be 3.4 nm from the  $E^{1/2}$  dependence.
- 11) S. I. Raider, R. Flitsch, and M. J. Palmer, *J. Electrochem. Soc.*, **122**, 413 (1975).
- 12) C. R. Brundle, H. Hopster, and J. D. Swalen, *J. Chem. Phys.*, **70**, 5190 (1979).